Coupling DTI and histological analysis to examine the multiple layers of the human fetal brain cerebral wall

Hao Huang[1], Tina Jeon[1], and Linda J. Richards[2]

[1]*Advanced Imaging Research Center, University of Texas Southwestern Medical Center, Dallas, TX, United States,* [2]*The Queesland Brain Institute, The University of Queesland, Brisbane, Queesland, Australia*

Target Audience: The MR physicists, clinicians and neuroscientists interested in coupling high resolution DTI and histology to understand underlying mechanism of DTI anisotropy in multiple layers of the developing fetal brains.

Introduction: The cerebral wall of human fetal brain is the place where active molecular and cellular activities take place during 2nd trimester fetal development, resulting in distinctive microstructures in different layers. These microstructural differences of the layers can be distinguished with the high contract from DTI-derived fractional anisotropy (FA) map (e.g. 1). As a complementary approach, various histological staining identified multiple layers of the human fetal brain cerebral wall (e.g. 2-3) and revealed microstructural configuration of different layers with much higher resolution than DTI. Coupling DTI and histology provides the insight on understanding the underlying microstructural configuration differences of FA measurements at different layers. In this study, high resolution DTI data from postmortem 2nd trimester human fetal brain were acquired. After DTI, these brains were stained with hematoxylin or immunohistochemically labeled with anti-glial fibrillary acidic protein (GFAP) antibody and neurofilament (NF) antibody. Using the regions of interests (ROIs) from the corresponding histological sections, differential FA values across the cerebral wall layers were quantified.

Methods

High resolution DTI of postmortem human fetal brain in 2nd trimester: Two to three samples at each week from 13 to 22 weeks of gestation (wg) were obtained from a tissue bank. For diffusion tensor imaging, 3D multiple spin echo diffusion tensor sequence was applied with 11.7T and 4.7T Bruker systems and following parameters: TE=35ms, TR=0.8s, FOV=37-54mm/28-53mm/28-37mm, imaging matrix=128×80×80, b=1000s/mm^2. *Histology:* After DTI data acquisition, sections of some fixed postmortem brains were rinsed in PBS before they were blocked in 2% normal goat serum. After they were stained with hematoxylin, or immunohistochemically labeled with GFAP antibody and NF antibody, the sections were mounted onto gelatinized glass slides, dehydrated through increasing concentrations of ethanol, immersed in two changes of Histo-Clear solution, and coverslipped with DPX mounting medium. *Histology-DTI correlation:* For a selected histological image, a corresponding coronal or axial slice of DTI image was chosen to match the histological section after rotation of the 3D DTI data. FA quantification of the small segments of cerebral wall corresponding to those from GFAP and NF histological images were based on a manual selection of regions of interest (ROIs). We further segmented three layers, namely cortical plate, subplate and inner layer from cortical plate to ventricle, with the contrasts observed from hemotoxylin-stained section of a 15wg brain. The segmentation based on hematoxylin-stained histological image was mapped to corresponding FA map with large deformation diffeomorphic metric mapping (LDDMM, 4).

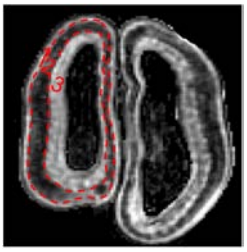

Fig. 1: Three layers from the pial surface to the ventricle are the cortical plate (designated layer 1), subplate (designated layer 2) and the inner layer (designated layer 3), and can be clearly identified with the FA map of a typical second trimester fetal brain at 17wg.

Results

Three layers in the cerebral wall delineated by DTI: As shown in the FA map in Fig. 1, three layers can be clearly differentiated in most regions of the cerebral wall. They are the cortical plate, subplate and an inner layer. The inner layer can be further differentiated into multiple zones with histology (2), namely the intermediate zone (fetal white matter), the subventricular zone, the periventricular zone and the ventricular zone. *Coupling DTI and histology to study all three layers:* With co-registered coronal histological image (Fig. 2a) and the FA map (Fig. 2c) of the 15wg brain after LDDMM transformation, the measurements revealed significant differences of FA values among these layers (Fig. 2f) with the ROIs determined by histology (Fig. 2b). Highest FA in the cortical plate is related to the clearly visible radial architecture with the enlarged histological image (Fig. 2d and 2e). *Coupling DTI and histology to study inner layer:* The FA values in the inner layer reflect integrated effects of the microstructures of multiple zones within the inner layer. GFAP staining in Fig. 3a and neurofilament staining in Fig. 3e revealed both radial (Fig. 3a) and tangential (Fig. 3e) microstructures, respectively. The radial microstructures are apparent close to the ventricle (Fig. 3b). The tangential structures in Fig. 3f delineate the fetal white matter axonal fibers and appear only in part of the inner layer, which is likely to be intermediate zone. Combined with the observation from Fig. 3b and 3f, it is possible that there are perpendicular crossings of radial and tangential fibers in this part of the layer 3. Due to these crossings, the FA values at the ROI (Fig. 3c and 3d) with predominantly radial structures are significantly higher (Fig. 3i) than those at the ROI (Fig. 3g and 3h) with mixed tangential and radial fibers.

Fig. 2 (left): The highly organized layer 1 or cortical plate in hematoxylin-stained histological section is characterized by the highest FA value among all layers in the cerebral wall. (a) is an image of a hematoxylin-stained histological section of a 15wg fetal brain. (d) shows a magnified image of the boxed region of (a). (e) shows a further magnified image of the boxed region in (d). Radial microstructures in the cortical plate are clearly visible in (e), indicated by yellow lines. (b) shows the segmentation based on contrast of histological image (a), dividing the cerebral wall into three layers. These layers, layer 1, layer 2 and layer 3, match cortical plate, subplate and inner layer differentiated from the FA map. (c) is the co-registered FA map after LDDMM transformation. (f) shows the FA measurements of these three layers. CP in (e) is the abbreviation of cortical plate. Asterisks in (f) indicate p less than 0.001.

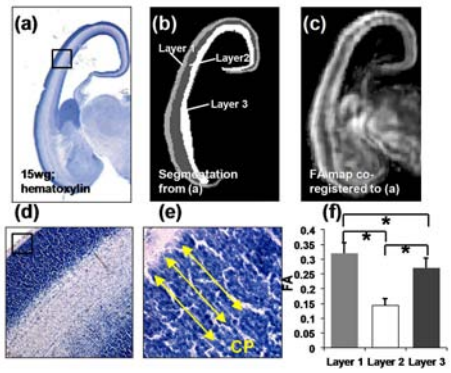

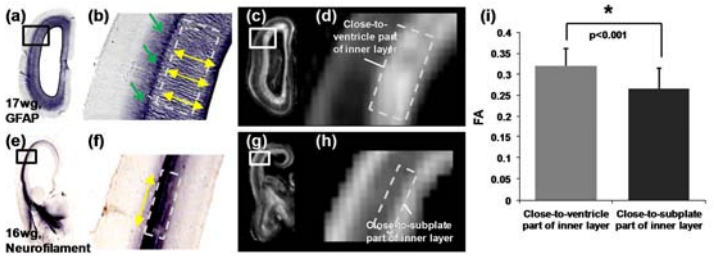

Fig. 3 (right): GFAP histological (a, b) image of a 17wg fetal brain and the corresponding FA maps (c, d) are shown in the upper panel. The close-to-ventricle part of inner layer (layer 3) has clear radial fibers in GFAP images (a, b). Neurofilament histology image of 16wg fetal brain and corresponding FA maps (g, h) are shown in the lower panel. Tangential fibers can be observed in the close-to-subplate part of inner layer (layer 3). The ROIs for FA measurements in (i) are shown in (d) and (h) as dashed boxes, which are consistent with those derived from histology contrasts in (b) and (f), respectively. Yellow lines in (b) and (f) indicate the orientations of the microstructures. Green lines in (b) point to the region where GFAP stain color changes and possibly the crossing of tangential and radial fibers takes place.

Discussion and conclusion

Highest FA values were found in the cortical plate rather than fetal white matter. The crossing of tangential and unmyelinated fetal white matter and radial glial may have contributed to even lower FA values in fetal white matter layer (intermediate zone) than the closest subventricular and periventricular zone. Coupling DTI and multiple staining from histology provides the insights on qualitatively and quantitatively characterizing the details of microstructures in the cerebral wall of human fetal brain.

References: [1] Maas et al (2004) Neuroimage 22, 1134. [2] Kostovic et al (2002) Cereb Cortex 12:536. [3] Vasung et al (2010) J Anat 217, 400. [4] Miller et al (2002) Annu Rev Biomed Eng 4, 375.

Acknowledgement: This study is sponsored by NIH MH092535 and NIH EB009545.